N90-18983

POSITRON ANNIHILATION IN GAMMA-RAY BURSTS

Alice K. Harding
Laboratory for High Energy Astrophysics
NASA/Goddard Space Flight Center
Greenbelt, MD

ABSTRACT

Emission features appear at energies of 350 - 450 keV in the spectra of a number of gamma-ray burst sources. These features have been interpreted as electron-positron annihilation lines, redshifted by the gravitational field near the surface of a neutron star. Evidence that gamma-ray bursts originate at neutron stars with magnetic field strengths of $\approx 10^{12}$ Gauss has come from recent observations of cyclotron scattering harmonics in the spectra of two bursts. Positrons could be produced in gamma-ray burst sources either by photon-photon pair production or by one-photon pair production in a strong magnetic field. The annihilation of positrons is affected by the presence of a strong neutron star magnetic field in several ways. The relaxation of transverse momentum conservation causes an intrinsic broadening of the two-photon annihilation line and there is a decrease in the annihilation cross section below the free-space value. An additional channel for one-photon annihilation also becomes possible in high magnetic fields. The physics of pair production and annihilation near strongly magnetized neutron stars will be reviewed. Results from a self-consistent model for non-thermal synchrotron radiation and pair annihilation are beginning to identify the conditions required to produce observable annihilation features from strongly magnetized plasmas.

INTRODUCTION

Gamma-ray bursts (GRBs) are transient sources of gamma rays having remarkably little ($\approx 1\%$) of their emission below 1 keV (for complete review see Ref. 1). They were discovered by the Vela satellite in 1969, though not recognized as events of cosmic origin until 1973, during a search for gamma-ray transients correlated with supernovae[2]. Early spectra showed smooth shapes which resembled the emission of tenuous, hot plasmas with temperatures of a few hundred keV. Since then, each new generation of gamma-ray detectors has discovered more bursts, revealing new and unanticipated characteristics of these sources. The Soviet KONUS experiments on the Venera satellites observed a large number of bursts, many of which showed evidence of absorption and emission lines[3]. The absorption dips occur around 20 - 40 keV and were interpreted as cyclotron absorption or scattering in magnetic fields of $2-5\times10^{12}$ Gauss. The reality of these features has been recently confirmed by detectors with higher resolution on the GINGA satellite[4]. Emission features at energies around 350 - 450 keV appear in about $10\%-20\%$ of the GRBs observed by KONUS and may be electron-positron annihilation radiation, redshifted in the gravitational field of a neutron star.

Although gamma-ray burst sources have been studied by astrophysicists for over fifteen years, their origin is still a mystery. One outstanding problem which has impeded theoretical progress is the lack of information on GRB distances. The energy of a typical burst as derived from the observed fluence, $E_B \approx 10^{38}\,\mathrm{erg\,(d/1kpc)^2}$, could reasonably be anywhere in the range, $10^{34}-10^{44}$ erg. Fortunately, the situation is not completely unresolved, as there now exist several strong lines

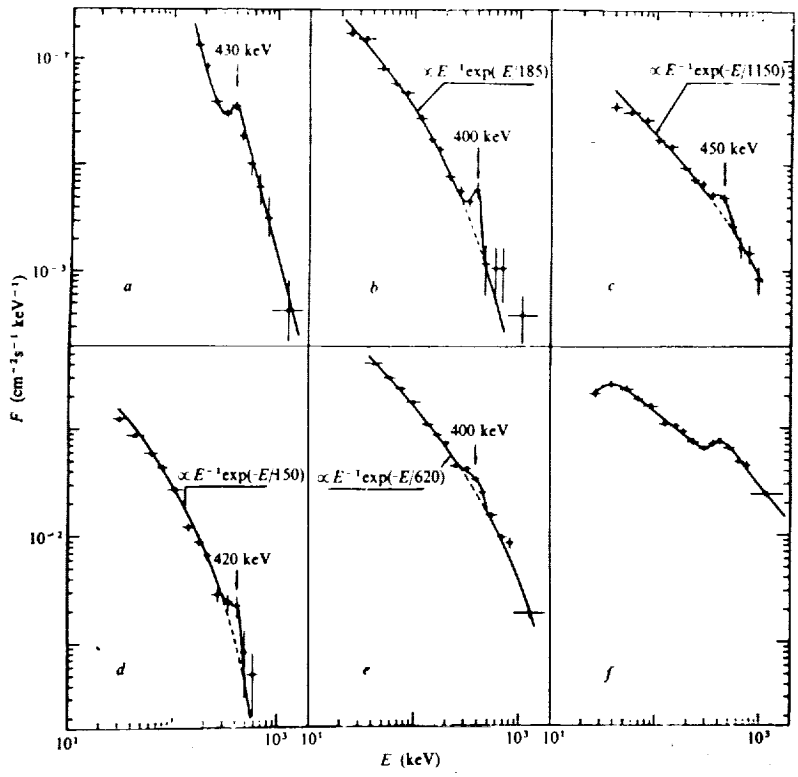

Fig. 1 - Photon spectra from the KONUS gamma-ray burst data base, fitted with narrow emission features (from Ref. 3).

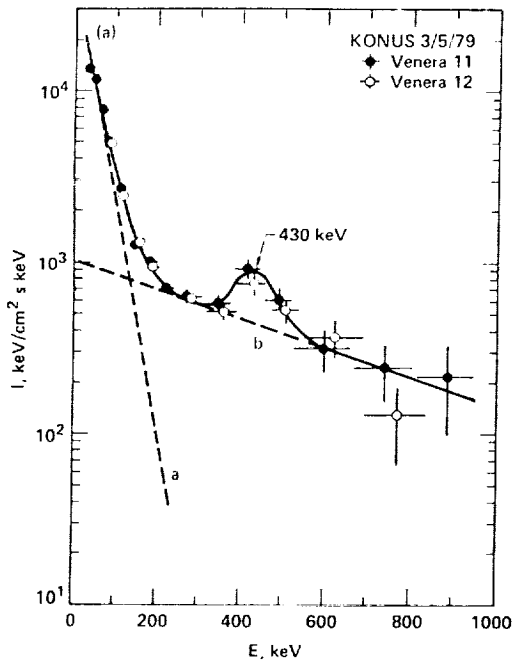

Fig. 2 - Spectrum of 1979 Mar. 5 burst from KONUS, showing annihilation feature at 430 keV (from Refs. 9 and 14).

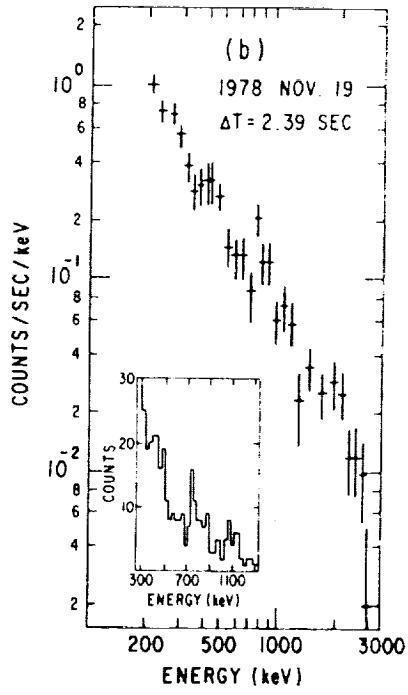

Fig. 3 - Count spectrum of 1978 Nov. 19 burst from the ISEE-3 Ge spectrometer, showing possible annihilation feature at 420 keV (from Ref. 8).

of evidence linking GRBs to neutron stars. The observed emission features, if identified as positron annihilation at rest, have redshifts in the range expected for a neutron star surface gravitational potential. The discovery of a very intense burst on March 5, 1979 had a rise time less than 0.2 ms, restricting the source size to less than 60 km, and also showed 8 second pulsations during the burst decay phase. The spectrum of this source also showed the strongest annihilation feature observed to date. Finally, the GINGA satellite has observed strong absorption features at 20 and 40 keV in the spectra of two bursts[4]. The most natural interpretation of the features is that they are harmonics of resonant cyclotron scattering in a field of 1.7×10^{12} Gauss[5–7], further indication of a neutron star origin.

The evidence that GRBs originate near strongly magnetized neutron stars allows us to model the emission processes, even if we do not know the ultimate source of the burst energy. It is likely that the strong magnetic field will profoundly influence the physical processes which produce the observed emission. In particular, the physics governing positron production and annihilation is so different from the corresponding free-space physics that new models for positron annihilation lines must be developed for GRBs. Ultimately, these kinds of emission models may lead to limits on the total burst energy required to produce observable annihilation features, thus imposing limits on GRB distances.

OBSERVATIONAL EVIDENCE FOR ANNIHILATION FEATURES

Evidence for positron annihilation in GRBs first appeared in data from the Ge spectrometer on the ISEE-3 satellite and from the KONUS detector on the Venera satellites. Figure 1 shows several examples of spectra obtained by KONUS with suggestions of features around 400 keV. The most convincing evidence for an annihilation line in a GRB spectrum was seen in the burst of Mar 5, 1979 (GB790305). Although this exceptionally strong burst was actually detected by nine different satellites, the best spectrum was obtained by KONUS (Figures 1a and 2) and shows a symmetric feature at 430 ± 30 keV which clearly stands out above the continuum. The feature has a relatively high statistical significance of 4.9σ. Observations of GB790305 by the French-Soviet SIGNE detector revealed that a large fraction of the excess at 430 keV came during the first 24 ms of the burst[10], providing some confirmation of the reality of the feature. Figure 3 shows the ISEE-3 spectrum of a burst with an emission feature at 420 keV and another possible feature at 738 keV. The higher energy feature is consistent with ^{56}Fe line emission at 847 keV, with the same redshift required for an annihilation line interpretation of the 420 keV feature.

There are, however, several problems connected with these observed emission features which require caution in interpreting them as annihilation lines. First of all, many of the lines are of low statistical significance (around 3σ) and the problem is compounded by the nature of the response functions of gamma-ray detectors. Since these instruments actually detect the energy loss rather than the energy of the gamma rays, the count rate spectra cannot be unfolded to yield a unique photon spectrum of the burst. The traditional technique has been to assume a spectral shape (in the case of the KONUS spectra, a thermal bremsstrahlung continuum plus a Gaussian line) and unfold the count spectrum, varying a set of adjustable parameters until an acceptable fit is achieved. Thus, the appearance of a line feature in the photon spectrum (especially one which is statistically marginal) can depend on the assumed continuum shape and the derived photon spectrum even tends to conform to the assumed input spectrum. This "obliging" nature of the data which can actually cause artificial amplification of a line feature in the photon spectrum, has raised doubts about many

of the reported features[11]. However, a number of these features also appear in the raw count spectra and some of the reported lines, especially the strong feature appearing in the spectrum of the Mar. 5, 1979 burst, *are* statistically significant.

The second problem is that other instruments, notably the Gamma-Ray Spectrometer on the Solar Maximum Mission (SMM), did not detect line features in *any* of their GRB spectra[12], including several of the same bursts showing emission features in the KONUS spectra. A possible resolution to this discrepancy is that the various detectors integrate over different time intervals to obtain burst spectra. If the lines are in fact time variable, then a detector with a shorter integration time could detect a line which would be averaged out over longer times. Actually, the emission features *do* appear to be variable over very short timescales. The SIGNE detector[13] reported an annihilation "flash" as short as their time resolution of 250 ms in the same burst from which SMM reported no line feature in a 16 s integration.

To summarize, there is convincing evidence from several instruments for annihilation lines in GRB spectra with the following general properties: 1) All of the reported features have redshifts in the range $\Delta E/E \simeq 0.2 - 0.5$, which are consistent with the softer neutron star equations of state[14]. This implies that positrons annihilate near a neutron star surface and probably in a strong magnetic field. 2) In most cases, the lines are so narrow (≤ 250 keV) that the required pair temperatures are much lower than the continuum temperatures[15]. In other cases, the features can be fit with broad line profiles ($\sim 0.5 - 1$ MeV) which may contribute significantly to the continuum above the line[16]. 3) The energy in the line represents typically around 10% and up to as much as 30% of the burst energy. 4) The annihilation features appear to be variable on timescales short compared to the total burst duration and are strongest near the peak of the burst.

POSITRON PRODUCTION AND ANNIHILATION PHYSICS

If the annihilation lines in GRBs originate at the neutron star surface, the theory of their formation must include the effects of the strong magnetic field on the physics of positron production and annihilation. Magnetic fields affect physical processes in several fundamental ways. Momentum perpendicular to the field direction is quantized, so that electrons and positrons must occupy discrete Landau states with energy

$$E_n = (m^2 + p^2 + 2nm^2B')^{1/2} \tag{1}$$

where $n = l + \frac{1}{2}(s+1) = 0, 1, 2, \ldots$ with $l = 0, 1, 2, \ldots$. Particles may have either spin-up ($s = 1$) or spin-down ($s = -1$) along the field direction, except in the ground state $n = 0$, where only the spin-down state is allowed. The momentum component parallel to the field, p, is continuous and $B' = B/B_{\rm cr}$ is the magnetic field in units of the critical field, $B_{\rm cr} \equiv m^2c^3/e\hbar = 4.414 \times 10^{13}$ Gauss, in which the cyclotron energy equals the electron rest mass. Transverse momentum is not strictly conserved in interactions, because the magnetic field can absorb or supply momentum (parallel momentum and total energy *are* strictly conserved). Thus, a number of first order processes are allowed that are forbidden in free space. Among these are cyclotron radiation and absorption, familiar as classical electromagnetic processes in weak fields, as well as one-photon pair production and annihilation, which become important only in strong fields approaching $B_{\rm cr}$. In very strong fields, processes depend on the spin of the electrons and positrons, with the most important effect being the suppression of spin-flip channels.

In addition to the possibility of first-order processes, second-order processes may be strongly influenced by all of the above effects in a strong magnetic field. Therefore, the behavior of the cross sections for two-photon pair production and annihilation in the presence of a field must also be understood in order to correctly model GRB annihilation lines.

Positron Production Processes

Pair production is probably the most important positron production process in GRBs and in a strong magnetic field, pairs can be produced by one photon as well as by two photons. The attenuation rate for conversion of a single photon into an electron-positron pair in the presence of an external magnetic field (also referred to as magnetic pair production) was first calculated in the early fifties[17,18], but since this process is not possibly observable in laboratory fields, it did not receive much attention until the discovery of pulsars in the late sixties. In both processes, the electron and positron can be produced only in the discrete Landau states which are kinematically available. When the photon energy is near threshold, there may only be one or two of these states, and the cross sections will be resonant at each of the pair state thresholds.

Figure 4 shows the attenuation coefficient for one-photon pair production as a function of photon energy for $\theta = 90^0$, where θ is the angle of the photon direction with respect to the magnetic field. The threshold for producing a pair in the ground state is $2m/\sin\theta$. Although this resonance structure is important very near threshold, the increasing density of resonances with photon energy allows the use of a more convenient asymptotic expression when the number of available pair states becomes large ($\sim 10^3$). In this limit, the polarization-averaged attenuation coefficient for a photon of energy E_γ is[20]:

$$R_{1\gamma} = \begin{cases} 0.23\frac{\alpha}{\lambda\!\!\!^{-}}B'\sin\theta\exp\left(-\frac{4}{3\chi}\right) & \chi << 1 \\ 0.6\chi^{-1/3} & \chi >> 1 \end{cases} \tag{2}$$

where $\chi \equiv (E_\gamma/2m)B'\sin\theta$, α is the fine structure constant and $\lambda\!\!\!^{-}$ is the electron Compton wavelength. The probability of one-photon pair production thus rises exponentially with increasing photon energy and transverse field strength. This strong angular dependence has important consequences for photon transport in GRB models. A quick rule-of-thumb is that magnetic pair production will be important when the argument of the exponential in Eqn (2) approaches unity, or when $(E_\gamma/2m)B'\sin\theta \geq 0.1$. Consequently, near-threshold pair production becomes important when $B \sim 4 \times 10^{12}$ Gauss, so that in neutron star fields Eqn (2) must be corrected for threshold effects[19].

The two-photon pair production cross section in a strong magnetic field also has resonances near threshold due to the discreteness of the pair states[21]. The threshold depends on photon polarization direction with respect the field, with the lowest threshold condition taking the form[22]:

$$(E_1\sin\theta_1 + E_2\sin\theta_2)^2 + 2E_1E_2[1-\cos(\theta_1-\theta_2)] \geq 4m^2, \tag{3}$$

where E_1 and E_2 refer to the energies of the photons and θ_1 and θ_2 are their angles with respect to the field. The second term is the same as the free-space threshold condition and the first term appears as a result of nonconservation of perpendicular momentum. Thus it is possible for photons traveling parallel to each other ($\theta_1 = \theta_2 \neq 0^0$) to produce a pair, an event not permitted in free space.

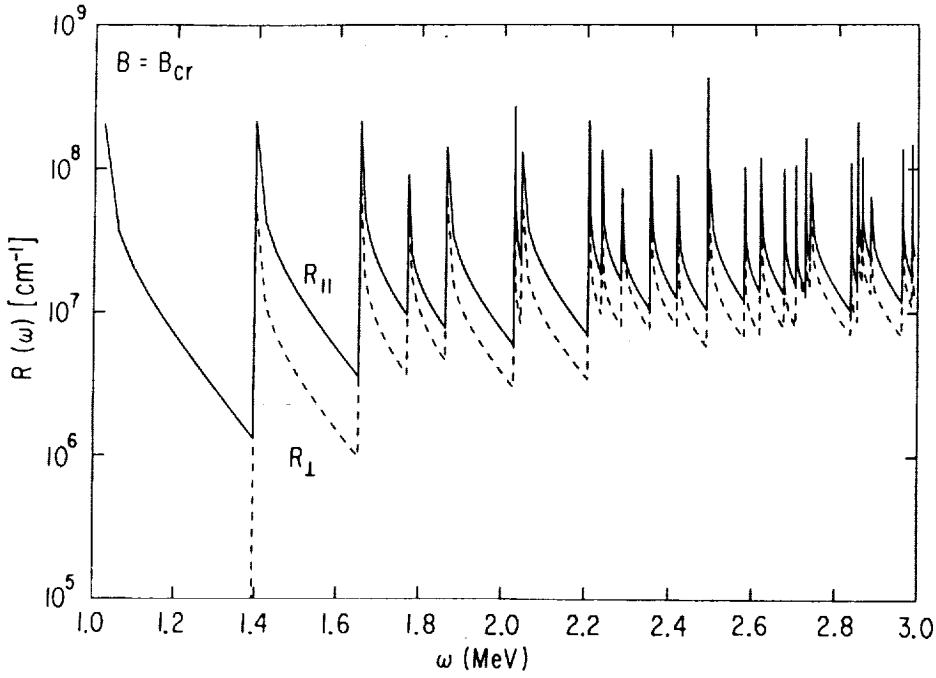

Fig. 4 - One-photon pair production attenuation coefficient as a function of photon energy, for photons propagating perpendicular to the field direction and with polarizations parallel and perpendicular to the field (from Ref. 19).

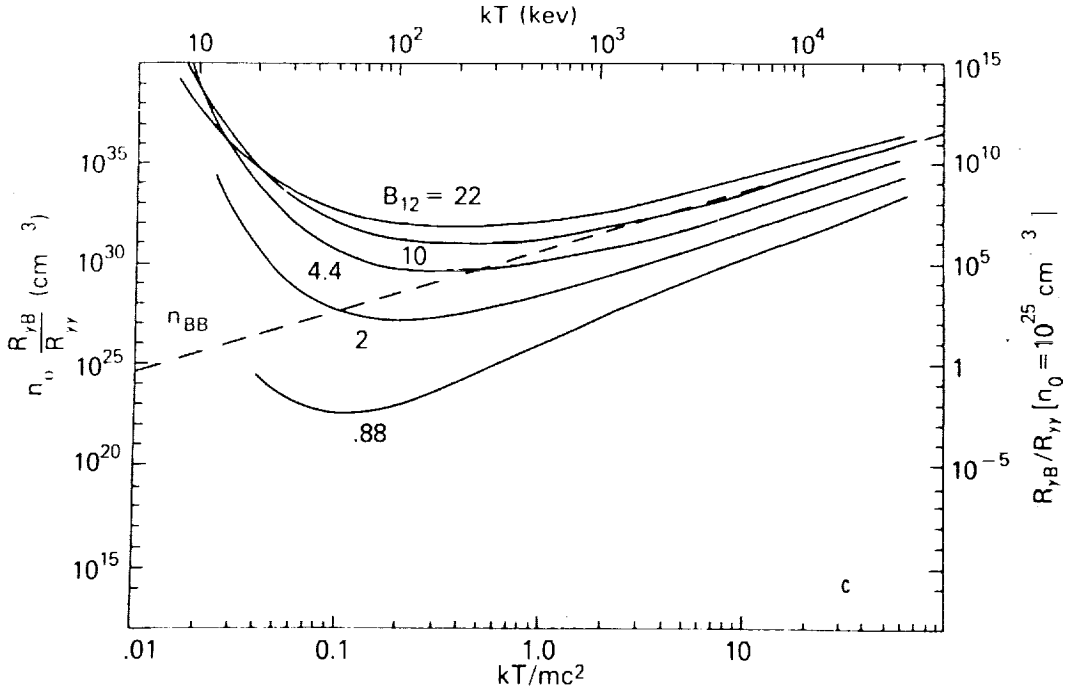

Fig. 5 - Ratio of one-photon to two-photon pair production rate vs. temperature for thermal synchrotron spectra. The curves are labeled with value of magnetic field strength in units of 10^{12} G (from Ref. 23).

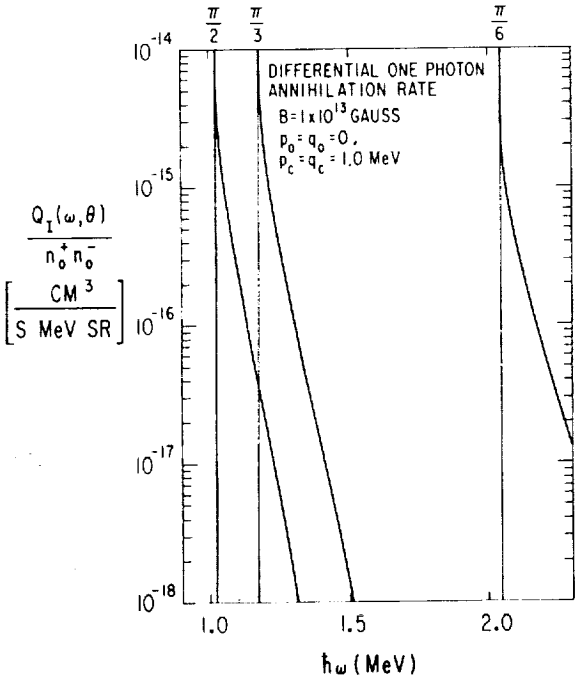

Fig. 6 - Differential one-photon annihilation spectrum emitted by ground state pairs with Gaussian parallel momentum distributions, here with widths of 1 MeV (from Ref. 22).

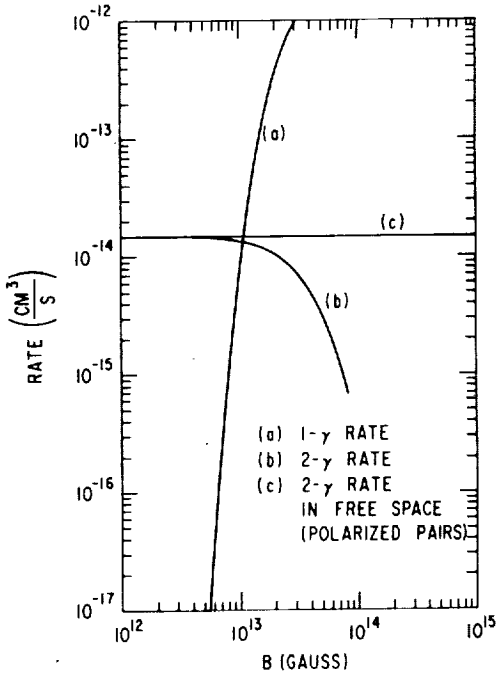

Fig. 7 - Comparison of the total rates for one and two photon annihilation at rest in the ground state, as a function of field strength. (from Ref. 22).

Because of the high photon densities and magnetic fields expected in GRB emission regions, one-photon and two-photon pair production will compete, and both will dominate over other positron production processes (e.g. radioactive decay). Figure 5 shows that in the case of a thermal synchrotron spectrum of photons with a density consistent with a GRB luminosity of $10^{38}\,\mathrm{erg\,s^{-1}}$, the one-photon process will generally dominate in magnetic fields above $\approx 10^{12}$ Gauss. It is probable then that, unless GRBs are more distant than 1 kpc, positrons will be created by one-photon pair production.

Positron Annihilation Processes

In a strong magnetic field, positrons may annihilate into one or two photons through the inverse of the pair production processes discussed above. Virtually all pairs annihilate directly rather than forming positronium at the temperatures and densities expected in GRB sources. Furthermore, because the synchrotron emission rates in fields $\approx 10^{12}$ Gauss ($\sim 10^{16}\,\mathrm{s^{-1}}$) are much larger than either collisional or annihilation rates, pairs are expected to cool to the ground state before annihilating.

One-photon annihilation from the ground state results in a line at $2m$, broadened asymmetrically by the parallel momenta of the pairs (cf. Figure 6). Unlike two-photon annihilation, Doppler broadening results only in a blueshift here, because the photon must take all of the kinetic energy of the pair in addition to the rest mass. The annihilation photons are emitted in a fan beam transverse to the field, which is broadened if the pairs have nonzero parallel momenta. Pairs annihilating from excited states would produce additional lines above 1 MeV which at high energies blend together into a continuum[24]. Figure 7 shows the one-photon and two-photon annihilation rates for pairs at rest in the ground Landau state. The one-photon rate increases exponentially with field strength, becoming comparable to the two-photon rate at around 10^{13} Gauss. The two-photon rate begins to decrease below the free-space rate at this same field strength, due to the smaller phase space of final pair states.

Two-photon annihilation results in a line at 511 keV as in free space, but the relaxation of transverse momentum conservation causes an additional broadening of the line at higher field strengths. For the case of annihilation of pairs at rest, the line is broadened by roughly $\Delta E \sim 4(B/10^{12}\ \mathrm{G})$ keV for emission parallel to $\mathbf{B}$ and $\Delta E \sim 54(B/10^{12}\ \mathrm{G})^{1/2}\sin\theta$ keV, $(\sin\theta > B'/2)$ for emission at angle θ to $\mathbf{B}$ (Ref. 22). In fact, there is an increasing tendency in very high fields for one of the photons to be produced with almost all of the pair energy, so that two-photon annihilation behaves more like one-photon annihilation. Widths of observed two-photon annihilation lines could in principle put limits on the magnetic field strength in GRBs. However, the widths of even the narrowest emission features observed in GRB spectra are too large (probably due to thermal broadening) to seriously constrain the magnetic fields by the above relations. The angular distribution of the photons from annihilation at rest also becomes more anisotropic with increasing field strength, with the peak of emission perpendicular to $\mathbf{B}$, again similar to one-photon annihilation.

NON-THERMAL PAIR ANNIHILATION MODEL

Given the evidence for annihilation line emission in observed GRB spectra, it seems natural to investigate under what conditions we would theoretically expect such line emission to be observable from a strongly magnetized neutron star. Thermal emission models (ie. bremsstrahlung or thermal

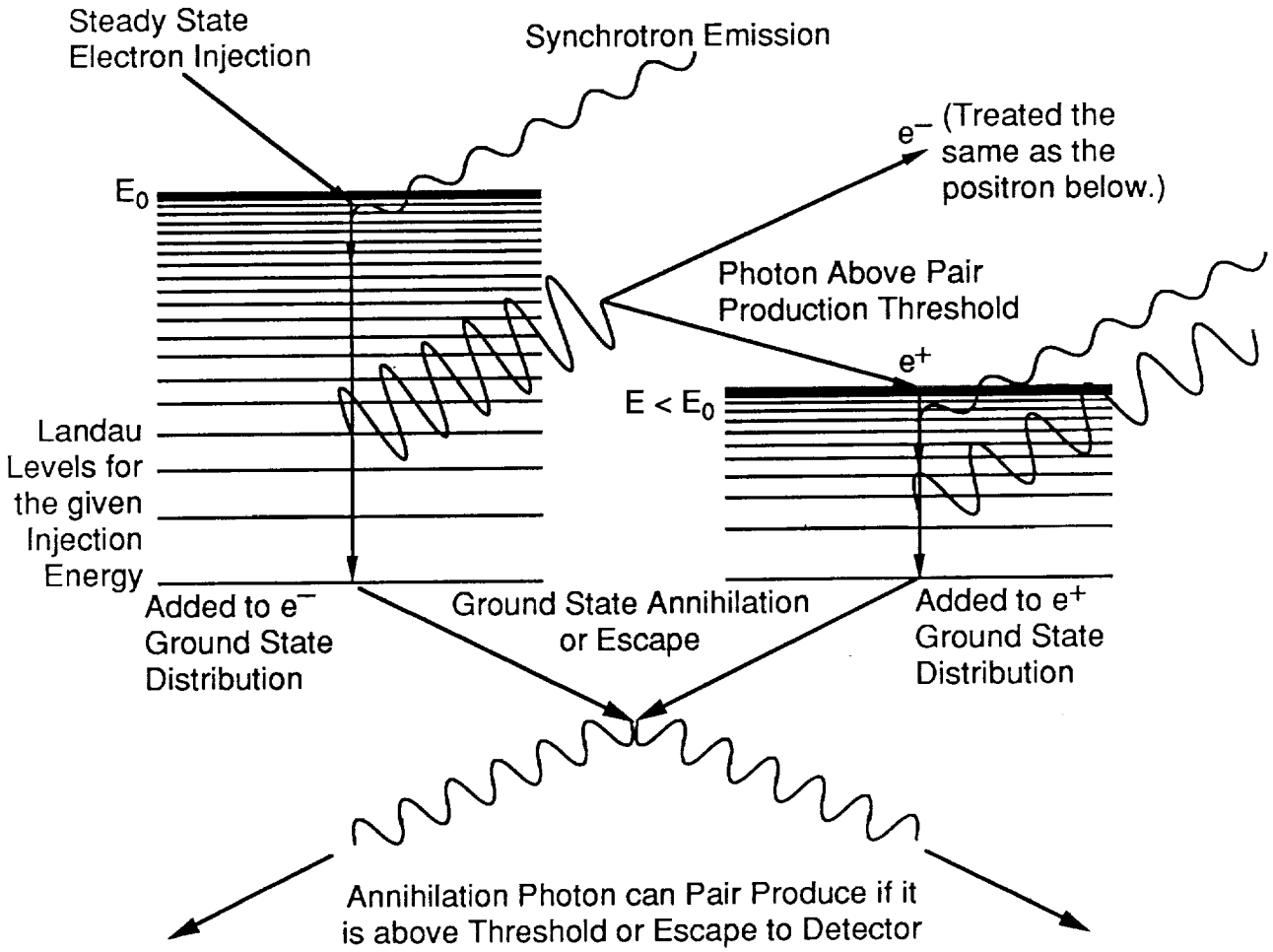

Fig. 8 - Schematic representation of nonthermal injection of energetic electrons in a strong magnetic field.

synchrotron) originally provided good fits to the early GRB continuum spectra. However, when the SMM detector obtained a number of GRB spectra showing hard power-law emission extending well above 1 MeV (Ref. 25), thermal models were questioned. A number of theoretical problems have also caused thermal models to fall out of favor: the inconsistency of annihilation line widths with continuum "temperatures" mentioned earlier, the difficulty of maintaining a thermal distribution of radiating particles in a strong magnetic field, and studies indicating that thermal pair-equilibrium plasmas do not yield observable annihilation features[26,27]. Thus, nonthermal emission models for GRBs seem more attractive.

The question of whether nonthermal injection of energetic electrons into a strong magnetic field can result in observable annihilation lines through the production of a dense electron-positron pair plasma is currently being investigated[28]. The photon emission spectrum is calculated by means of a Monte Carlo simulation. Figure 8 shows schematically the different processes involved in such a calculation. Electrons are injected with an assumed distribution of energy and pitch angle into a homogeneous, strong field. The polar angle, energy and spin of the injected electron determine its initial Landau state, characterized by (n, s, p). Since synchrotron radiation rates are very high, the electron quickly cascades down a series of Landau states to the ground state. Spin-dependent, quantum synchrotron transition rates, interpolated from tables, are used to determine the series of radiative transitions. The synchrotron photons above magnetic pair production threshold may create pairs in excited states. These particles are treated the same as the injected electrons and their synchrotron photons contribute both to the observed spectrum and to the production of additional pairs. As injection continues, particles accumulate in the ground state and either annihilate or escape. The free-space two-photon annihilation rate (valid as long as $B < 10^{13}$ G) is calculated from the annihilation cross section averaged over the ground state distribution. The differential cross section is used to determine the angle of one of the annihilation photons with respect to the field direction. The angle of the second photon and both photon energies follow from three-dimensional kinematics.

To obtain self-consistent electron and positron distribution functions in the ground state, the lifetime of each annihilating or escaping particle is used to calculate the density in the momentum bin of the particle. The newly calculated density replaces the current density value for that momentum and the process is repeated until convergence of the entire spectrum of particles is achieved. Compton scattering of pairs in the ground state with synchrotron photons prior to annihilation or escape may also be important in determining the steady-state particle spectrum, but is not yet included in the calculation.

Examples of the steady-state photon and pair spectra resulting from simulations with varying input parameters are shown in Figures 9 - 11. Each figure represents a large number ($\sim$ 30,000) of injected primary electrons and the photon distributions are differential spectra per primary. In each spectrum, photons from primary synchrotron emission (light solid line), pair synchrotron emission (dot-dashed line) and annihilation radiation (dashed line) are shown separately. The heavy solid line is the sum of the three contributions to the total spectrum. Self-consistent pair density distributions included with each spectrum are normalized to a density, $n_o \equiv (q_o/\sigma_T c)^{1/2}$, where q_o is the rate of injection per second per unit volume of primary electrons and σ_T is the Thomson cross section. In the case of monoenergetic injection of electrons with energy E_o, q_o is related to the total luminosity L and source size R by $q_o = L/(E_o R^3)$. In the simulations shown in Figs. 9 - 11, the value of R determines the relative importance of escape and annihilation and was assumed to be 10^6 cm.

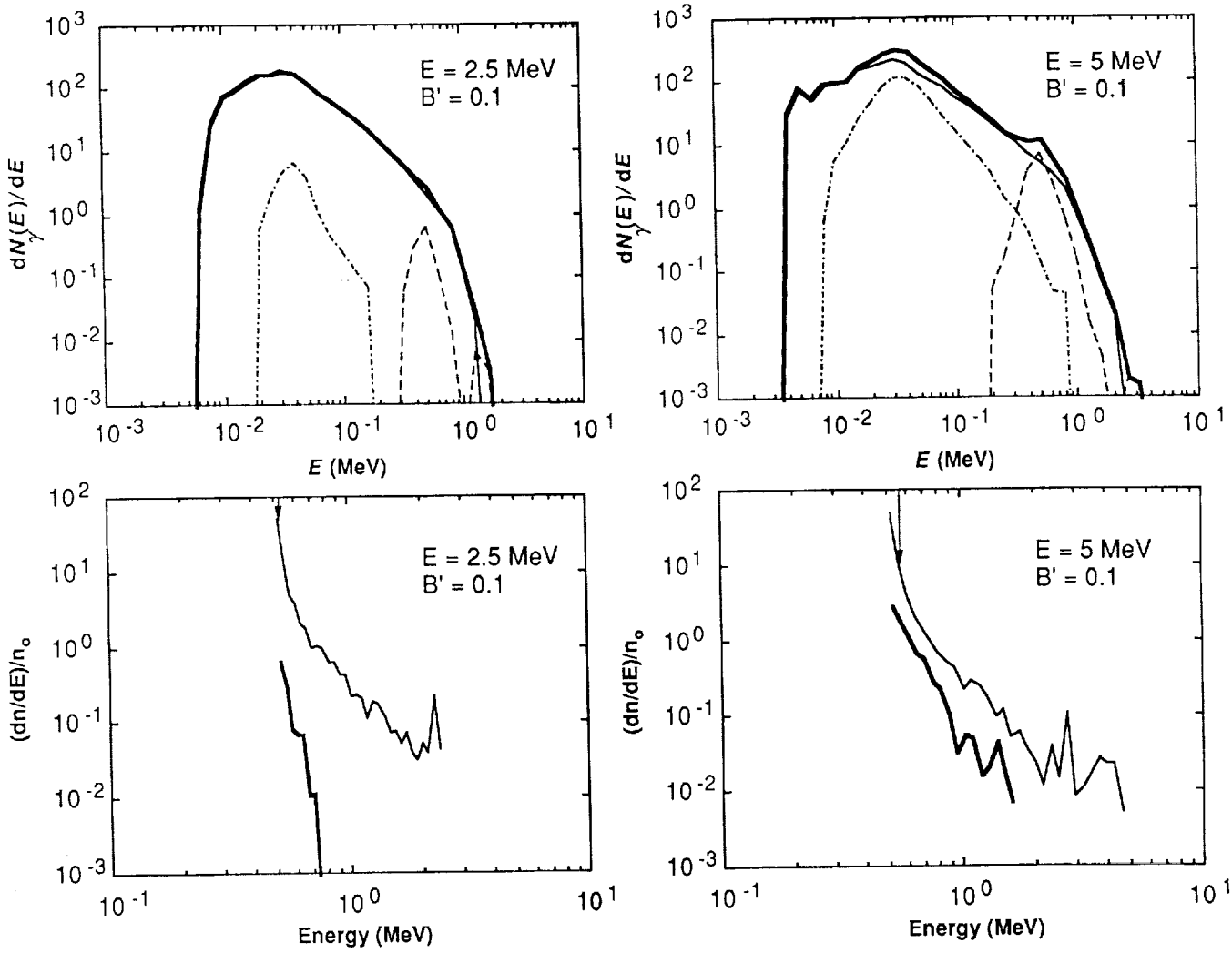

Fig. 9 - (Top) Angle-averaged photon number spectra for isotropic, monoenergetic injection in a 0.1 B_{cr} field. The light solid line is the synchrotron emission from primaries only, the dot-dashed line is synchrotron emission from created pairs, the dashed line is annihilation radiation and the dark solid line is the total spectrum. (Bottom) Self-consistent pair density distribution functions vs. energy for the same case as above. The light solid line corresponds to the electrons and the dark solid line corresponds to the positrons. The arrow indicates the point which divides the electrons that annihilate (to the left) from those that escape (to the right) (From Ref. 28).

As can be seen from these examples, an annihilation feature is visible above the continuum for a variety of parameters. Figure 9 shows the steady-state photon and pair spectra which result from a monoenergetic, isotropic injection of unpolarized primary electrons. The continuum spectra display the -3/2 power law shape of synchrotron cooling emission above the cyclotron energy $E_c = mB'$, with cutoffs above 1 MeV due to pair production. Harmonic structure due to transitions between very high, closely-spaced Landau states can be seen at the low energy end of the spectra. Synchrotron cooling emission from the pairs produced in excited states contributes most strongly around the cyclotron energy, because more pairs are produced in lower Landau states. The annihilation lines are roughly symmetric about the 511 keV peak (gravitational redshift has not been included), with power-law wings. Annihilation photons also undergo pair production attenuation, but since most of these photons are beamed along field lines, the threshold lies well above 1 MeV. As the field strength increases, so does the width of the annihilation line for a given injection energy. The widths of the lines range from a few hundred keV to roughly 1 MeV. At a given field strength, increasing the injection energy increases the strength of the annihilation feature.

The steady-state pair distributions have a power law shape at high energies with steep increase in density near rest. Since only electrons are being injected in these simulations and positrons come only from pair production, some of the electrons must escape rather than annihilating. The arrows mark the energy above which most electrons escape. The steepening of the pair spectra at low energies are thus caused by the energy dependence of the annihilation rate. As the magnetic field strength increases, the higher pair production rates cause the positron spectra to approach that of the electrons, both in shape and amplitude.

In these simulations, the annihilation features are fairly narrow. Synchrotron radiation cools primarily transverse to the field, but the pairs still have sufficient parallel momenta in the ground state to produce much broader annihilation lines. However, when the annihilation rate is compared with the escape rate for electrons as a function of energy, one sees that annihilation occurs preferentially near rest, with the rate dropping very fast with increasing parallel momentum. Therefore, the lines are narrow when the higher energy electrons escape and do not contribute to the Doppler broadening of the annihilation. This situation occurs when the average number of pairs produced per primary is less than unity (*i.e.* the plasma is not pair dominated).

Beamed injection of primaries in a cone along the magnetic field or in a fan beam across the field has also been investigated. The cone beam results in a decrease of pair production and the fan beam in an increase in pair production over isotropic injection. Cone-beamed injection (Figure 10) produces pair distributions not only with lower density but having peaks above rest energy, causing the annihilation feature to be considerably weaker. On the other hand, fan-beamed injection (Figure 11) produces exceptionally strong, narrow annihilation features, not only because of the increase in pairs, but because of the steepening of the steady-state pair spectra (*i.e.* more pairs can annihilate near rest). The continuum spectra in these cases have very sharp pair production cutoffs at 1 MeV.

From the results of these simulations, observable annihilation lines can result from steady-state, nonthermal injection of electrons in a strong magnetic field. It requires field strengths of at least $B' \sim .05$, injection energy of at least 5 MeV and a large fraction of primaries with high transverse momentum. The escape of higher energy electrons along the magnetic field is important and can result in narrow annihilation lines. The simultaneous production of strong, narrow annihilation features and hard power-law emission above 1 MeV seems to be difficult in this model. However,

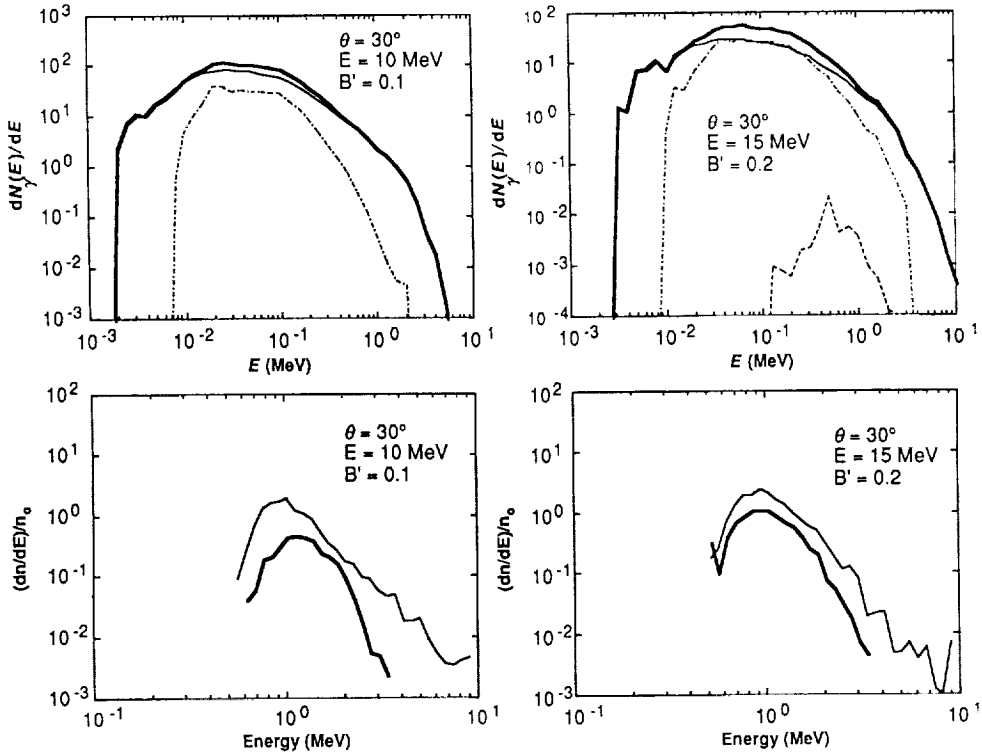

Fig. 10 - Same as Fig. 9, for cone-beamed, monoenergetic injection. Escape dominates annihilation at all energies in the electron distribution function.

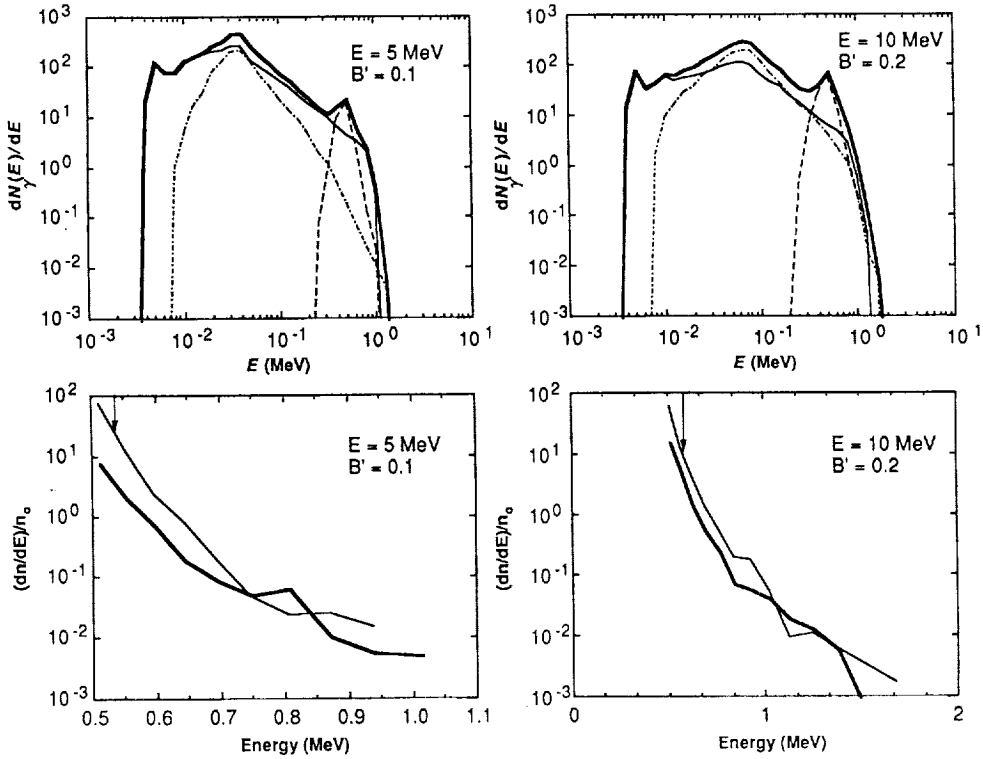

Fig. 11 - Same as Fig. 9, for fan-beamed, monoenergetic injection.

time variability of both the line and high-energy continuum could arise from changes in either the energy or the angular distribution of the injected electrons.

SUMMARY

Although the models for pair annihilation in GRBs are now including more of the physics of high magnetic fields, they are still in a fairly primitive state of sophistication. Inhomogeneity and spatial dependence have not been considered; and the inclusion of additional processes such as two-photon pair production and Compton scattering introduce new levels of complexity in the simulation codes. For example, the resonant nature of Compton scattering in a strong magnetic field is difficult to include in full detail, though the essential physics may be possible to include approximately. Nevertheless, the results of even the simplest models are beginning to identify the conditions under which observable pair annihilation can occur.

The experimental situation is expected to improve in the near future with the launch of new instruments on the Gamma-Ray Observatory. The Burst and Transient Source Experiment (BATSE) will have unprecedented sensitivity for performing spectral observations and temporal variability studies of GRBs. With time resolution as short as $10\mu s$, BATSE will be able to study the time variability of annihilation features during a burst and make a 5σ detection of a line feature with 20% equivalent width from a strong burst in less than a second[29]. Most importantly, the issue of whether positron annihilation is actually occuring in GRBs may finally be resolved.

ACKNOWLEDGEMENTS

I am grateful to my collaborators J. K. Daugherty and R. D. Preece for hard work and many fruitful discussions. I also thank R. W. Bussard, M. G. Baring, and D. Q. Lamb for helpful comments and insights.

REFERENCES

1. Liang, E. P. and Petrosian, V. 1986, *Gamma-Ray Bursts* (AIP: New York).
2. Klebesadel, R., Strong, I. and Olson, R. 1973, *Ap. J. Letters*, **182**, L85.
3. Mazets, E. P. *et al.* 1981, *Nature*, **290**, 378.
4. Murakami, T. *et al.* 1988, *Nature*, **335**, 234.
5. Lamb, D. Q. *et al.* 1989, *Proc. 14th Texas Symposium on Relativistic Astrophysics*, ed. E. Fenyves, in press.
6. Fenimore, E. E. *et al.*, 1988, *Ap. J. Letters*, **335**, L71.
7. Harding, A. K. and Preece, R. D. 1989, *Ap. J. Letters*, **338**, L21.
8. Teegarden, B. J. and Cline, T. L. 1980, *Ap. J. Letters*, **236**, L67.
9. Mazets, E. P. *et al.* 1979, *Nature*, **282**, 589.
10. Cline T. L. 1984, *High Energy Transients in Astrophysics*, ed. S. E. Woosley, (AIP: New York), p. 333.
11. Fenimore, E. E. *et al.* 1982, *Gamma-Ray Transients and Related Astrophysical Phenomena*, ed. R. E. Lingenfelter, (AIP: NewYork), p. 201.
12. Nolan, P. L. *et al.* 1983, *Electron-Positron Pairs in Astrophsyics*, ed. M. L. Burns, A. K. Harding

and R. Ramaty, (AIP: New York), p. 59.
13. Barat, C., Hurley, K. Niel, M. and Vedrenne, G. 1984, *Ap. J. Letters*, **286**, L11.
14. Liang, E. P. 1986, *Ap. J.*, **304**, 682.
15. Ramaty, R. and Meszaros, P. 1981, *Ap. J.*, **250**, 384.
16. Golenetskii, S. V. *et al.* 1986, *Astrophys. Space Sci.*, **124**, 243.
17. Toll, J. S. 1952, Ph. D. Thesis, Princeton Univ., unpublished.
18. Klepikov, N. P. 1954, *Zh. Eksp. Teor. Fiz.*, **26**, 19.
19. Daugherty, J. K. and Harding, A. K. 1983, *Ap. J.*, **273**, 761.
20. Erber, T. 1966, *Rev. Mod. Phys.*, **38**, 626.
21. Kozlenkov, A. A. and Mitrofanov, I. G. 1987, *Sov. Phys. JETP*, **64**, 1173.
22. Daugherty, J. K. and Bussard, R. W. 1980, *Ap. J.*, **238**, 296.
23. Burns, M. L. and Harding, A. K. 1984, *Ap. J.*, **285**, 747.
24. Harding, A. K. 1986, *Ap. J.*, **300**, 167.
25. Matz, S. M. *et al.* 1985, *Ap. J. Letters*, **288**, L37.
26. Zdziarski, A. A. 1984, *Ap. J.*, **283**, 842.
27. Harding, A. K. 1984, *Proc. of Varenna Workshop on Plasma Astrophysics*, (ESA SP-207), p. 205.
28. Preece, R. D. and Harding, A. K. 1989, *Ap. J.*, (Dec. 15) in press.
29. Fishman, G. J. *et al.* 1989, *Proc. of GRO Science Workshop*, in press.